

Diastereodifferentiating the [2+2] Photocycloaddition of Ethylene to Arylmenthyl Cyclohexenonecarboxylates: Stacking-Driven Enhancement of the Product Diastereoselectivity That Is Correlated with the Reactant Ellipticity

Ken Tsutsumi,^[a] Yuuki Yanagisawa,^[a] Akinori Furutani,^[a] Tsumoru Morimoto,^[a] Kiyomi Kakiuchi,^{*,[a]} Takehiko Wada,^[b] Tadashi Mori,^[c] and Yoshihisa Inoue^{*,[c]}

Abstract: Upon diastereodifferentiating the [2+2] photocycloaddition of ethylene to a series of *p*-substituted (–)-8-phenylmenthyl cyclohexenonecarboxylates, the diastereoselectivity was critically controlled by the nature of the substituent introduced to the chiral auxiliary, and the *p*-nitro-substituted substrate afforded the cycloadducts in 90% diastereomeric excess

(*de*) and with 97% isolated yield. Detailed experimental and theoretical conformation analyses revealed that the stacking interaction of the aromatic auxiliary with the cyclohexenone

Keywords: chirality • circular dichroism • diastereoselectivity • ethylene • photocycloaddition

moiety plays the decisive role in determining the substrate conformation and is, therefore, responsible for the dramatic enhancement of the *de*. Of particular interest, the product *de* was directly related to the ellipticity of the substrate, enabling us to “predict” the *de* prior to photoirradiation.

Introduction

Photochemical [2+2] cycloaddition constitutes an important and versatile synthetic method for the construction of complex (poly)cyclic molecules.^[1] Recent progress in chiral photochemistry has driven us to develop reliable synthetic routes to asymmetric photocycloaddition, because the photocycloadducts obtained are often valuable precursors to biologically active natural products, such as terpenoids with polyquinane skeletons.^[2] Our and other groups have investi-

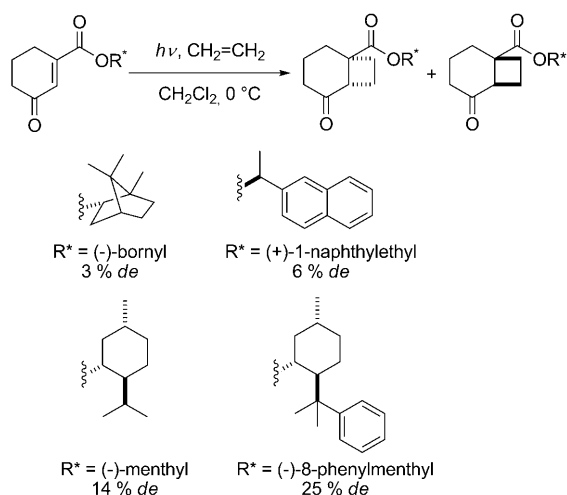
gated a range of asymmetric [2+2] photocycloadditions to reveal that the diastereodifferentiating photoreaction using chiral auxiliaries is one of the most promising methods for asymmetric induction.^[3,4] So far, we have examined a variety of chiral auxiliaries in the diastereoselective [2+2] photocycloaddition of cyclohexenones to the smallest olefin, ethylene, and found that menthyl derivatives are the most effective chiral auxiliaries for obtaining [2+2] photoadducts in high diastereomeric excesses (Scheme 1).^[4]

Chiral menthyl auxiliaries have been widely applied not only to photoreactions but also to various thermal reactions,^[5] such as Michael additions,^[6] radical reactions,^[7] Diels–Alder reactions,^[8] and Friedel–Crafts reactions.^[9] However, little is known about the factors and mechanisms operating in the asymmetric induction process, in particular the roles of the aromatic substituent introduced to the menthyl auxiliary. In the present study, to gain deeper insights into the mechanism of chiral induction, we systematically investigated the diastereodifferentiating [2+2] photocycloaddition of ethylene to cyclohexenones modified with a series of chiral *p*-substituted 8-phenylmenthyl auxiliaries. The original conformations in the ground state, which are believed to control the subsequent photochemical asymmetric induction, were elucidated through X-ray crystallographic and circular dichroism (CD) spectral analyses as well as

[a] Dr. K. Tsutsumi, Y. Yanagisawa, Dr. A. Furutani, Dr. T. Morimoto, Prof. K. Kakiuchi
Graduate School of Materials Science
Nara Institute of Science and Technology (NAIST)
Takayama, Ikoma, Nara 630-0101 (Japan)
Fax: (+81) 743 72 6089
E-mail: kakiuchi@ms.naist.jp

[b] Prof. T. Wada
Institute of Multidisciplinary Research for
Advanced Materials, Tohoku University
2-1-1 Katahira, Aoba-ku, Sendai 980-8577 (Japan)

[c] Dr. T. Mori, Prof. Y. Inoue
Department of Applied Chemistry, Osaka University
2-1 Yamada-oka, Suita 565-0871 (Japan)
Fax: (+81) 6 6879 7923
E-mail: inoue@chem.eng.osaka-u.ac.jp



Scheme 1. Diastereoselective [2+2] photocycloaddition of ethylene to cyclohexenones.

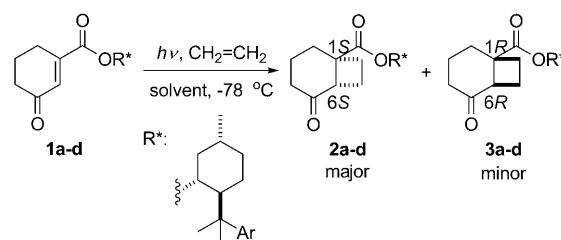
theoretical calculations. We further attempted to correlate the magnitude of the observed Cotton effect of the starting material with the diastereoselectivities of the photocycloadduct obtained.

Results and Discussion

Diastereodifferentiating the photocycloaddition of cyclohexenonecarboxylates **1 with ethylene:** The diastereodifferentiating [2+2] photocycloadditions of a series of (–)-8-(*p*-substituted-phenyl)menthyl-modified cyclohexenone carboxylates (**1a–d**) were performed under comparable conditions to elucidate the roles of the aryl substituent introduced to the menthyl moiety. The preparations of substrates **1a**, **1c**, and **1d** have been reported,^[4,10] and the new chiral cyclohexenone **1b** with the (–)-8-(4-isopropylphenyl)menthyl auxiliary was prepared by using a modified version of the reported procedure.^[4,10] The photoreaction was carried out in a variety of solvents at –78 or –40 °C by irradiating an ethylene-saturated solution of **1** in a Pyrex flask at wavelengths of >280 nm with a 500 W high-pressure mercury lamp, and the products were analyzed by NMR spectroscopy.

The results are summarized in Table 1. The photoreaction proceeded smoothly in each solvent to give two diastereomeric isomers **2** and **3** in high isolated yields, whereas the diastereoselectivity turned out to depend critically on the substituent introduced and the solvent used. The absolute configuration of the major photoadduct **2** was determined unequivocally as 1*S*,6*S* by a direct comparison with the X-ray crystallographic structure of the major photoadduct obtained from a related compound.^[11] The NMR spectral feature of **2** is similar to that of the compound. In addition, we transformed **2** into the methyl ester derivative according to the literature procedure^[11] and obtained a similar optical rotation to that obtained for a specimen obtained from a menthyl ester of which the configuration had been unambig-

Table 1. Diastereoselective [2+2] photocycloaddition of ethylene to cyclohexenonecarboxylates **1a–d** with chiral 8-arylmenthyl auxiliaries at –78 or –40 °C^[a]



	Ar	Solvent	Yield [%] ^[b]	de [%] ^[c]
1 ^[d]		CH ₂ Cl ₂	84	40
2		toluene	87	55
3		MCH ^[e]	86	44
	1a			
4		CH ₂ Cl ₂	96	24
5		toluene	99	41
6		MCH ^[e]	86	22
	1b			
7 ^[d]		CH ₂ Cl ₂	95	50
8 ^[d]		toluene	99	75
9 ^[d]		MCH ^[e]	96	81
	1c			
10 ^[f]		CH ₂ Cl ₂	94	88
11 ^[f]		toluene	92	81
12 ^[g]		toluene	100	75
13 ^[h]		MCH ^[e]	86	82
14 ^[g]		MeCN	97	90
	1d			

[a] A 0.05 M solution of **1** in each solvent was purged with ethylene at 25 °C for 5 min and then irradiated under an ethylene atmosphere at –78 or –40 °C in a Pyrex flask (>280 nm), by using a 500 W high-pressure Hg lamp as the light source. [b] Isolated yield by column chromatography on silica gel. [c] Determined by ¹H NMR spectroscopy. [d] Reference [4]. [e] MCH: methylcyclohexane. [f] Reference [10]. [g] At –40 °C. [h] 0.005 M.

uously derived from an X-ray structure determination previously.^[11]

Cyclohexenone **1a** bearing the phenylmenthyl auxiliary gave the photoadducts with a moderate diastereomeric excess (*de*) of 40–55% in dichloromethane, toluene, and methylcyclohexane (MCH; see Table 1, entries 1–3). Introduction of a bulky isopropyl substituent at the *para*-position of the phenyl ring in **1b** significantly reduced the *de* (to 22–41%) in all the solvents examined (entries 4–6). In contrast, the use of the (4-methoxyphenyl)menthyl auxiliary in **1c** (entries 7–9) considerably enhanced the diastereoselectivity with a clear tendency for increasing diastereoselectivity with decreasing solvent polarity, thus affording moderate (50%) *de* in dichloromethane but much better (81%) *de* in MCH. Interestingly, the 4-nitrophenyl derivative **1d** afforded the photoadducts in high chemical (>86%) and optical yields (>81% *de*) at –78 °C, irrespective of the solvent used (entries 10–13). In particular, the best result (97% yield and 90% *de*) was obtained in polar acetonitrile at –40 °C (entry 14); note that the reaction temperature was higher than that (–78 °C) used for the other solvents due to the higher freezing point of acetonitrile.

Theoretical calculation of the conformer distribution of **1**:

The presence and population of conformers of the starting material **1** in the ground state can affect the diastereoselectivity of the photocycloaddition. Although the cyclohexane ring of the menthol moiety is fixed in the chair form, there are at least four major conformations for **1** associated with the rotations around the menthol's C2–C8 bond and the cyclohexenone–carbonyl bond, the former of which leads to stacked and unstacked (axial and *trans*) conformers and the latter (s)-*cis* and (s)-*trans* conformers, as illustrated in Figure 1. Thus, the conformer distributions were calculated

by the relative stability of the major conformers in the ground state. The relative energies and the Boltzmann distributions of the most stable ST and SC conformers were calculated by the DFT method at the B3LYP 6-31G* level to give the results shown in Table 2.^[12]

The energy differences are about 2.0–6.7 kJ mol^{−1} in favor of the ST conformer. There is a good correlation between the Boltzmann distribution and the *de* values. Thus, the substrate with larger energy difference provides a higher *de* value, and **1d** gives the largest relative energy and the best diastereoselectivity.

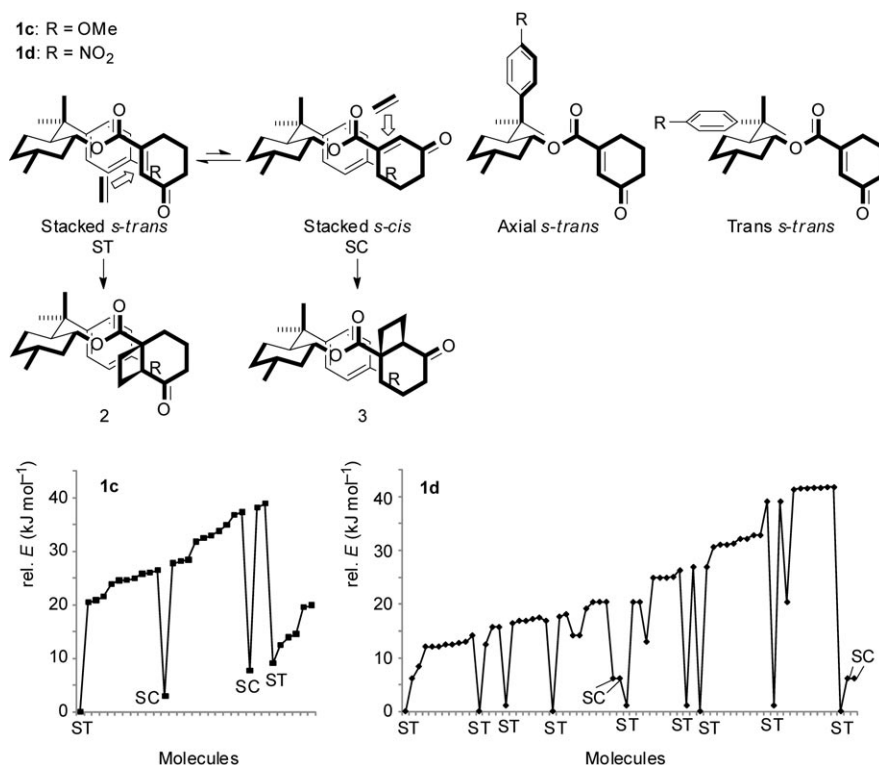


Figure 1. Conformer distributions of **1c** and **1d** based on MMFF calculations.

for **1c** and **1d** by the MMFF method.^[12] The results of the calculation indicate that the stacked conformers, in which the cyclohexenone ring and the aromatic ring are located face-to-face, are more stable than the unstacked ones. Of the four major conformations, the stacked (s)-*trans* (ST) is the most stable, which is in accord with the results obtained in our previous studies.^[4]

The ST conformer affords the (1*S*,6*S*)-isomer **2** upon photocycloaddition to ethylene since the aromatic ring shields the *re*-face of cyclohexenyl ring and the photoreaction is faster than the bond rotation. On the contrary, the SC conformer is presumed to yield the (1*R*,6*R*)-isomer **3**. In our previous single crystal X-ray crystallographic study, we revealed that the major diastereomer of a related photoadduct possesses the 1*S*,6*S* configuration.^[11] Since **2** is of 1*S*,6*S* configuration, it is likely therefore that the diastereodifferentiation upon photocycloaddition is directly manipulated or af-

X-ray crystallographic analyses of **1a–d**:

To obtain the experimental support for the stable conformer, X-ray crystallographic analyses were performed for single crystals of **1a–d** (Figure 2). All of the X-ray structures obtained reveal that the ST conformer is the most stable among others. Furthermore, the C1–C3 and to a lesser extent the C2–C4 distance (Figure 2) are appreciably shorter for **1c** and **1d** than for **1a** and **1b** (Table 3), which is consistent with the higher conformational stability of the ST conformer (Table 2) as a consequence of the better stacking in **1c** and **1d**. We previously indicated that the electrostatic and/or dipole–dipole interactions between the C=O moiety of cyclohexenone and the OMe group attached to the aromatic ring could stabilize the ST con-

Table 2. Boltzmann distributions of the stable ST and SC conformers calculated by the DFT method at the B3LYP 6-31G* level.

Substrate	Relative energy ^[a] [kJ mol ^{−1}]	ST/SC ^[b]
1a	−2.000	64:34
1b	−2.412	73:27
1c	−2.983	82:18
1d	−6.673	94:6

[a] Value for the ST conformer based on the SC one as 0 kJ mol^{−1}.

[b] Boltzmann distribution.

formation of **1c**.^[4,10] In the case of **1d**, the intramolecular donor–acceptor interaction between the cyclohexenone's HOMO and the nitrophenyl's LUMO (Figure 3)^[12] may further stabilize the stacking conformation. It is reasonable therefore that these substrates, **1c** and **1d**, give the larger relative energies (Table 2) and the higher diastereoselectivity.

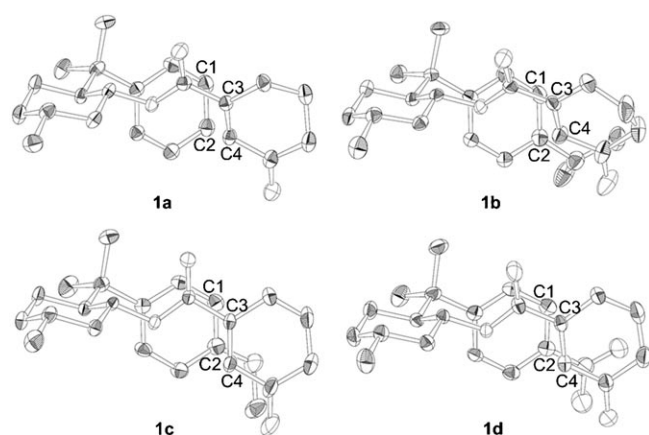
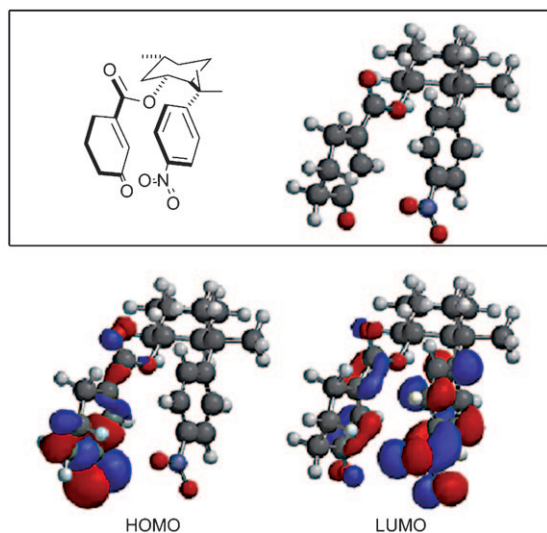
Figure 2. X-ray structures of **1a–d**.

Table 3. Distances between cyclohexenone's C3/C4 and phenyl's C1/C2.

Substrate	C1–C3 [Å]	C2–C4 [Å]
1a	4.24	3.72
1b	4.08	3.70
1c	3.71	3.68
1d	3.56	3.54

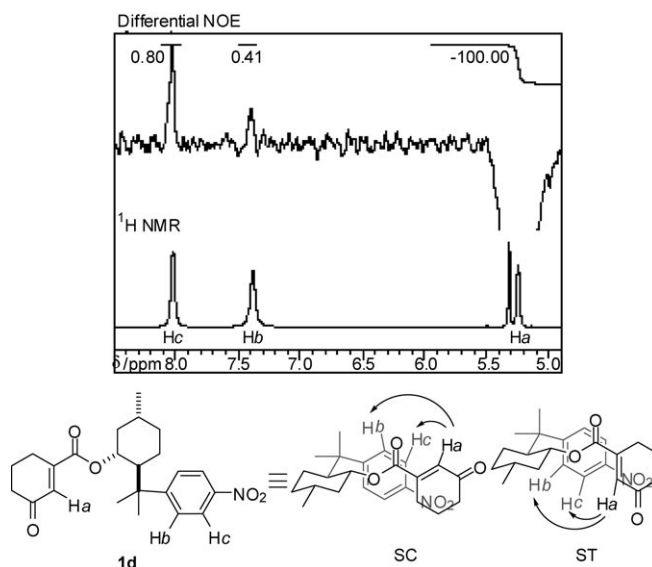
Figure 3. Molecular orbitals of **1d** calculated by the DFT method at the B3LYP 6-31G* level.

ties (Table 1) as a consequence of the better conformational stabilization through the donor–acceptor interactions.

NMR studies of 1a–d: The above theoretical calculations and the X-ray crystallographic data are in good agreement with the trend of the diastereoselectivity of the photocycloaddition. To obtain further experimental evidence for the stacking interactions in solution, we performed the conformational analyses of the starting materials **1** by using NMR

spectroscopy. In the ^1H NMR spectra measured in CDCl_3 , the olefinic proton signals of **1a–d** appeared at a significantly higher field than that of unsubstituted menthyl cyclohexenonecarboxylate **1e**.^[13] Thus, the olefinic peak appeared at $\delta = 6.13$ for **1a**,^[14] 6.34 for **1b**,^[15] 6.16 for **1c**,^[14] and 5.92 ppm for **1d**,^[14] which are significantly upfield-shifted from the original chemical shift at $\delta = 6.54$ ppm observed for **1e**.^[13] It is likely that the upfield shift of the olefinic protons is caused by the stacking of the cyclohexenone ring with the aromatic group in solution.

We further measured the differential NOE of **1d** in CD_2Cl_2 at -78°C . As shown in Figure 4, irradiation of the

Figure 4. ^1H NMR spectrum (differential NOE) of **1d** at -78°C .

olefinic proton *Ha* led to an NOE enhancement of the signal of aromatic protons *Hb* and *Hc* (*Hb*: 0.41, *Hc*: 0.80%). In contrast, no clear NOE was observed at RT. These results indicate that the enone moiety and the phenyl ring are located in close proximity or stacked to each other at low temperatures. The X-ray crystallographic analyses revealed that the *Ha–Hb* and *Ha–Hc* distances in the ST conformer of **1d** are 3.792 and 3.670 Å, respectively, which are short enough to observe the NOE. Some of the protons in the SC conformer are susceptible to NOE in its stacked form but not in the unstacked ones, and the fact that the NOE is more clearly observed at -78°C indicates that the stacked conformers are stabilized at lower temperatures, although the ST and SC conformers are difficult to unambiguously differentiate by the NMR spectroscopic analyses.

CD spectral analyses of 1: To obtain further insights into the ST and SC conformers, we measured the CD spectra of **1**. As shown in Figure 5, 8-phenylmenthyl ester **1a** gave an apparent exciton couplet at the major band, whereas menthyl ester **1e** and (–)-8-phenylmenthol exhibited only weak Cotton effects in the same region. This is reasonable, since

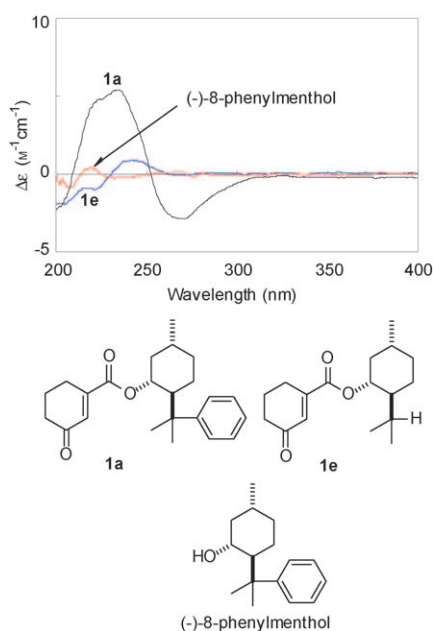


Figure 5. CD spectra of **1a**, **1e**, and (–)-8-phenylmenthol in methylocyclohexane at 25 °C.

only **1a** has two allowed π – π^* transitions in a molecule. The electric transition moments of the enone and phenyl chromophores are coupled spatially to each other to produce the strong intramolecular exciton coupling observed.

According to the exciton chirality theory,^[16] the helical sense of the spatial arrangement of two mutually coupling transition moments determines the sign of the observed exciton couplet. In the present case, the helical sense of the two transition moments are opposite to each other for the ST versus SC conformer, as illustrated in Figure 6. In the ST conformer, the two transition moments are positioned counter-clockwise to give a negative couplet, which means a negative–positive sequence in the CD sign from the longer wavelength. On the contrary, the two moments are twisted clockwise in the SC conformer to give a positive couplet. The negative exciton coupling observed for **1a** (Figure 5) indicates that the ST conformer is more dominant than the SC conformer, provided that the magnitude of the exciton coupling is comparable for both of the conformers.

Since the population of conformers is a critical function of the temperature in general, we measured the CD spectra of

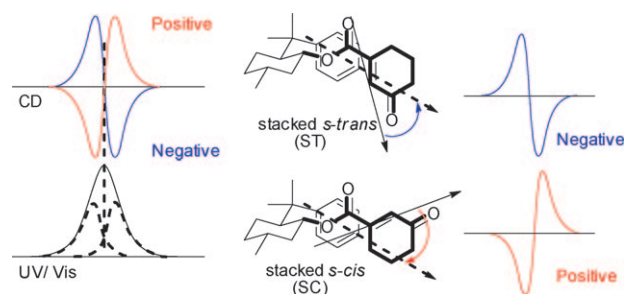


Figure 6. Excitonic CD spectrum model.

1a, **1b**, **1c**, and **1d** at varying temperatures (Figure 7). The CD spectra of **1a** showed a redshift with an appreciable intensity enhancement by lowering the temperature with an apparent isodichroic point (Figure 7a). Similarly, the CD intensity of **1b** was enhanced at low temperatures (Figure 7b). In the cases of **1c** and **1d**, a stronger negative exciton couplet was observed even at room temperature and the intensity was further increased with an apparent isodichroic point at lower temperatures (Figure 7c and d).

The UV/Vis spectra also showed similar but much smaller augmentation in intensity (Figure 8), which is attributable to the peak sharpening and the increased concentration due to the shrinking of the solution at low temperatures. To cancel the effect of the volume change, we calculated the anisotropy factor ($g = \Delta\epsilon/\epsilon$) by using the relevant CD and UV/Vis spectra obtained at each temperature. By using the g factor, which is free from the change in solution volume or substrate concentration, we can directly evaluate the effect of temperature on the conformation. As can be seen from Figure 8, the g factor of **1c** and **1d** significantly increases at lower temperatures, which indicates the increased population of the ST conformer. This CD spectral behaviour nicely

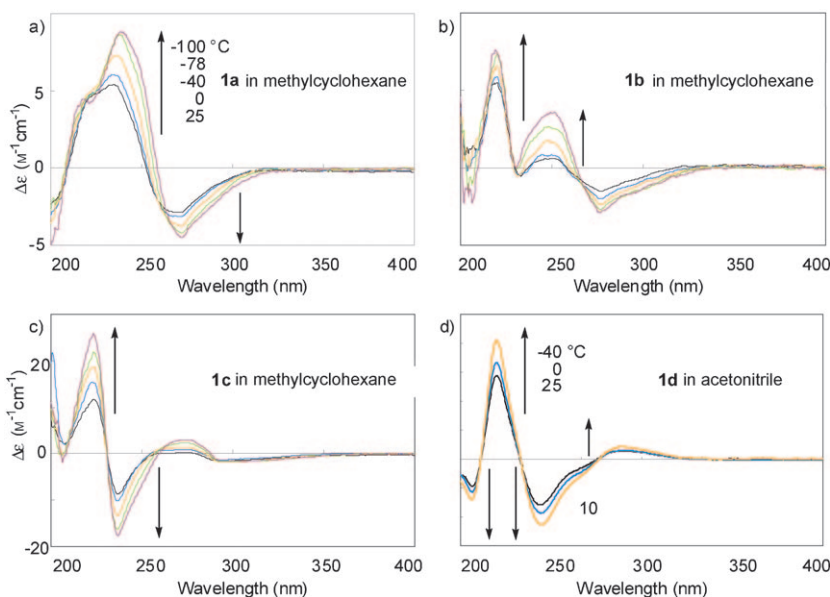


Figure 7. CD spectra of **1a–d** at 25, 0, –40, –78, and –100 °C.

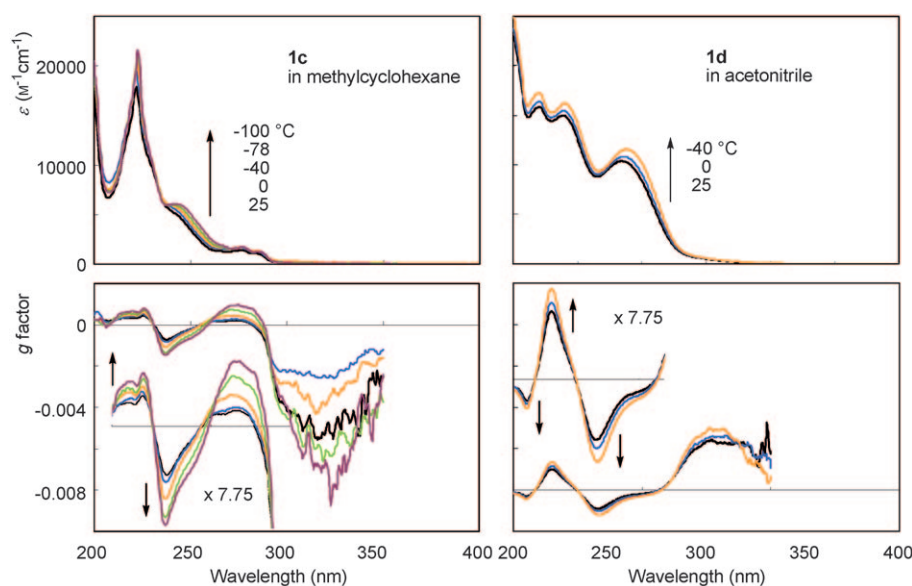


Figure 8. UV/Vis spectra (top) and g factor profiles (bottom) of **1c** and **1d** at 25, 0, –40, –78, and –100 °C (left) and in acetonitrile at 25, 0, and –40 °C (right).

coincides with the higher diastereoselectivities obtained in the photocycloaddition at lower temperatures.

Correlation between CD intensity and diastereoselectivity:

In the above discussion, we have elucidated that: 1) the aryl and cyclohexenone moieties of 8-arylmenthyl cyclohexenecarboxylates **1** are stacked to each other to form the ST or SC conformer, 2) the magnitude of the Cotton effect of **1** reflects the population of stacked ST and SC conformers, and 3) the conformer distribution in the ground state is the major source of the diastereoselectivity achieved in the subsequent photocycloaddition to ethylene. This scenario immediately prompted us to examine the correlation of the CD intensity of the starting material with the diastereoselectivity of the photoadduct obtained.

For this purpose, we employed **1c** and **1d** as representative substrates (as they gave the highest $\Delta\epsilon$ and de values), and their CD spectra were measured and the photoreactions were carried out at various temperatures to give the results summarized in Table 4. Both the $\Delta\epsilon$ and de values increased with decreasing temperature to reach the largest values at the lowest temperatures employed, that is, at –78 °C for **1c** and at –40 °C for **1d**. Interestingly, the plots of $\ln([2]/[3])$ against the $\Delta\epsilon$ value at each CD extrema gave good linear relationships, as shown in Figure 9. This indicates that the product's de obtained under a specific condition can be predicted by just measuring the CD spectrum of the substrate at least for **1c** and **1d**. Although the number of the applicable cases is rather limited in the present system, these are the first examples that reveal such a clear correlation between the substrate CD intensity and the product diastereoselectivity.

Conclusion

In summary, we found that the diastereoselectivity of the [2+2] photocycloaddition of cyclohexenone to ethylene can be enhanced by introducing a π – π stacking arylmenthyl auxiliary to cyclohexenone, which functions as a shield blocking the attack of ethylene from one of the diastereofaces of the cyclohexenone ring. The theoretical and CD spectral conformation analyses revealed that the stacked (*s*)-*trans* (ST) conformer is more stable than the stacked (*s*)-*cis* (SC) and other unstacked conformers, and is more populated at lower temperatures to give the photocy-

Table 4. The CD intensity $\Delta\epsilon$ of **1c** and **1d** and the diastereoselectivity of photoproducts obtained at various temperatures.

	Substrate	Solvent	<i>T</i> [°C]	λ_{ext} [nm]	$\Delta\epsilon$ [M ^{–1} cm ^{–1}]	Yield ^[a] [%]	$de^{[b]}$ [%]	$\ln([2]/[3])$
1	1c	MCH ^[c]	25	237	–8.7	59	33	0.686
2				223	11.7			
3				237	–10.2	32	49	1.072
4				223	15.4			
5	1d	MeCN	–40	237	–13.3	82	69	1.696
6				224	18.7			
7				237	–16.2	96	81	2.254
8				224	21.9			
9	1d	MeCN	25	266	–8.0	97	79	2.143
10				230	14.4			
11				210	–4.8			
12				266	–9.4	93	84	2.442
13	1d	MeCN	0	230	16.6			
14				210	–5.7			
15				267	–11.4	97	90	2.944
16				230	20.5			
17	1d	MeCN	–40	209	–7.1			

[a] Isolated yield by column chromatography on silica gel. [b] Determined by ¹H NMR spectroscopy. [c] MCH: methylcyclohexane.

cloadducts in higher diastereoselectivities of up to 90% de . A good linear relationship was found between the substrate CD intensity and the product de for a couple of strongly stacked substrates, enabling us to predict the diastereoselectivity from the CD spectral examination before performing the photoirradiation.

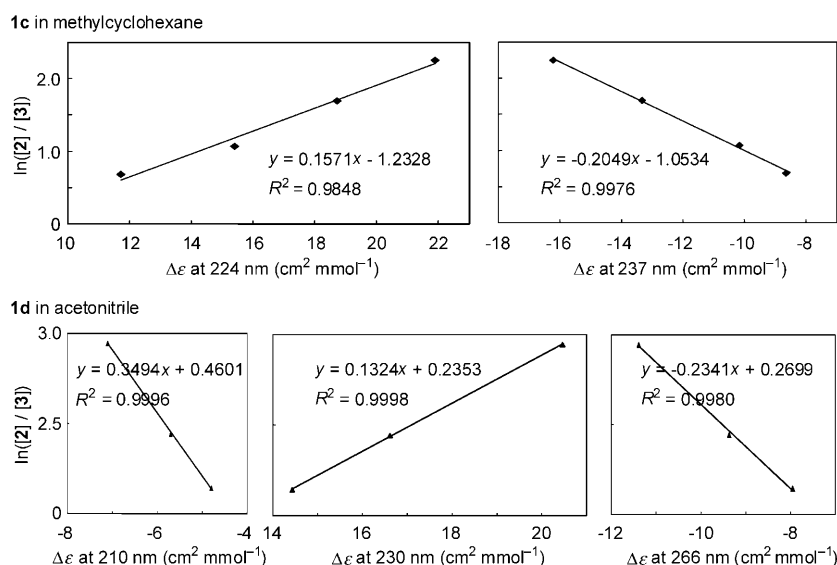


Figure 9. Plots of the logarithm of the diastereomeric ratio, $\ln([2]/[3])$, for **1c** and **1d** versus $\Delta\epsilon$ at varying wavelengths.

Experimental Section

General: Mostly commercially available reagents were used without further purification. All reactions and manipulations of air- and moisture-sensitive compounds were carried out under an atmosphere of dry nitrogen by using standard vacuum line techniques. Melting points were determined on a Yanaco MP-500D micro melting point apparatus. Optical rotations were determined on a JASCO DIP-1000 digital polarimeter by using the sodium D line. Infrared spectra (IR) were obtained on a JASCO FT/IR-420 spectrometer; absorption peaks are reported in reciprocal centimeters. High-resolution mass spectra (HRMS) were obtained on a JEOL JMS-700 instrument. Flash column chromatography was performed with Merck silica gel 60N. Proton nuclear magnetic resonance spectra (^1H NMR) and carbon nuclear magnetic resonance spectra (^{13}C NMR) were recorded on a JEOL JNM-ECP500 spectrometer. ^1H NMR spectra are reported as chemical shifts in parts-per-million (ppm) relative to tetramethylsilane (TMS) as the internal standard. Data are reported as follows: chemical shift in ppm (δ), multiplicity (s = singlet, d = doublet, t = triplet, q = quartet, td = triplet of doublet, brs = broad singlet, m = multiplet), coupling constant (Hz), and integration. ^{13}C NMR spectra are reported as chemical shifts in ppm based on the middle peak of CDCl_3 ($\delta = 77.0$ ppm), and signal assignments (s, d, t, and q) were made from DEPT experiments. High resolution mass spectra (HRMS) were obtained on a JOEL JMS-700. UV/Vis spectra were recorded on a SHIMADZU UV-1600PC UV/Vis spectrophotometer. CD specific rotations were measured in a 1 dm thermostated quartz cell on a JASCO J-720 polarimeter with PTC-348WI as a temperature control unit.

Syntheses of 1a–d: (–)-(1*R*,2*S*,5*R*)-5-Methyl-2-(1-methyl-1-phenylethyl)-cyclohexyl 3-oxo-1-cyclohexenecarboxylate (**1a**) was prepared according to Lange's procedure.^[3a,b] (–)-(1*R*,2*S*,5*R*)-5-Methyl-2-[1-methyl-1-(4-methoxyphenyl)ethyl]cyclohexyl 3-oxo-1-cyclohexenecarboxylate (**1c**) and (–)-(1*R*,2*S*,5*R*)-5-methyl-2-[2-(4-nitrophenyl)propan-2-yl]cyclohexyl-3-oxo-1-cyclohexenecarboxylate (**1d**) were prepared according to literature procedures.^[4,10]

(–)-(1*R*,2*S*,5*R*)-2-[2-(2-Isopropylphenyl)propan-2-yl]-5-methylcyclohexyl 3-oxo-1-cyclohexenecarboxylate (**1b**): 1,3-Dicyclohexylcarbodiimide (DCC; 2.64 g, 12.8 mmol) was added to a mixture of 3-oxo-1-cyclohexenecarboxylic acid (0.66 g, 4.7 mmol), (+)-(*R*)-8-(4-isopropylphenyl)menthol (1.17 g, 4.3 mmol), and dimethylaminopyridine (DMAP; 0.21 g, 1.7 mmol) in dry CH_2Cl_2 (21 mL) at 0°C. The mixture was stirred for 5 min at that temperature and then for 2.5 h at room temperature. The

precipitated dicyclohexylurea was removed by filtration through a glass filter, and the filtrate was washed with 0.5*N* HCl and then with a saturated aqueous solution of NaHCO_3 . During this procedure, additional precipitated dicyclohexylurea was again removed by filtration of both layers to facilitate their separation. The organic layer was dried (MgSO_4) and concentrated in vacuo. The residue was purified by flash chromatography (AcOEt /hexane 5:95) to give ester **1b** (1.45 g, 86%). Colorless solid; m.p. 89.0–90.9°C; $[\alpha]_D^{25} = -25.9$ ($c = 1.0$ in dichloromethane); IR (KBr): $\tilde{\nu} = 2959, 1713, 1688, 1229 \text{ cm}^{-1}$; ^1H NMR (500 MHz, CDCl_3 , 25°C, TMS): $\delta = 7.15$ (d, $J = 8.6$ Hz, 2H), 7.08 (d, $J = 8.6$ Hz, 2H), 6.34 (s, 1H), 4.99 (td, $J = 10.7, 4.3$ Hz, 1H), 2.84–2.79 (m, 1H), 2.36–2.26 (m, 3H), 2.10–2.07 (m, 2H), 1.93–1.88 (m, 2H), 1.86–1.83 (m, 1H), 1.78–1.73 (m, 1H), 1.69–1.65 (m, 1H), 1.55–1.48 (m, 1H), 1.29 (s, 3H), 1.21 (d, $J = 6.7$ Hz, 3H), 1.19 (d, $J = 6.7$ Hz, 3H), 1.18 (s, 3H), 1.11 (td, $J = 13.0, 3.3$ Hz, 1H), 1.01–0.86 ppm (m, 5H); ^{13}C NMR (126 MHz, CDCl_3 , 25°C, TMS): $\delta = 200.1$ (s), 165.5 (s), 149.3 (s), 148.7 (s), 145.3 (s), 132.4 (d), 125.9 (d, 2C), 125.1 (d, 2C), 75.7 (d), 50.2 (d), 41.7 (t), 39.0 (s), 37.6 (t), 34.5 (t), 33.2 (d), 31.3 (d), 28.5 (q), 26.6 (t), 24.8 (q), 24.3 (t), 24.1 (q), 23.7 (q), 22.1 (t), 21.7 ppm (q); HRMS (EI): m/z : calcd for $\text{C}_{26}\text{H}_{36}\text{O}_5$: 396.2664; found: 396.2666.

X-ray crystallographic analyses: Measurements were made on a Rigaku RAXIS-RAPID Imaging Plate diffractometer with MoK_α radiation at 296 K.

Compound 1b: $\text{C}_{26}\text{H}_{36}\text{O}_5$; colorless needle (0.40 × 0.20 × 0.18 mm); monoclinic; space group = $P2_1(\#4)$; $Z = 2$; $a = 6.140(4)$, $b = 19.964(12)$, $c = 9.593(5) \text{ \AA}$; $\beta = 96.06(2)^\circ$; $V = 1169.4(12) \text{ \AA}^3$; $\rho_{\text{calcd}} = 1.126 \text{ g cm}^{-3}$. Of 11323 reflections, up to $2\theta = 55.0^\circ$, 5307 were independent ($R_{\text{int}} = 0.039$) and 2603 with $I > 3.00\sigma(I)$. The structure was solved with direct methods and refined with full matrix against all F^2 data. Hydrogen atoms were calculated in "riding" positions. $wR = 0.0740$ and $R = 0.0580$.

Compound 1d: $\text{C}_{23}\text{H}_{29}\text{O}_5\text{N}$; colorless needle (0.40 × 0.17 × 0.10 mm); orthorhombic; space group = $P2_12_12_1(\#19)$; $Z = 4$; $a = 6.5573(3)$, $b = 15.6471(7)$, $c = 21.3024(9) \text{ \AA}$; $V = 2185.68(17) \text{ \AA}^3$; $\rho_{\text{calcd}} = 1.214 \text{ g cm}^{-3}$. Of 4804 reflections, up to $2\theta = 54.9^\circ$, 4804 were independent ($R_{\text{int}} = 0.000$) and 1815 with $I > 1.00\sigma(I)$. The structure was solved and refined in a manner analogous to **1b**. $wR2 = 0.0981$ and $R = 0.0574$. CCDC-766289 (**1b**) and -766290 (**1d**) contain the supplementary crystallographic data for this paper. These data can be obtained free of charge from The Cambridge Crystallographic Data Centre via www.ccdc.cam.ac.uk/data_request/cif.

Photoreaction of 1 with ethylene: Irradiations were carried out in a Pyrex flask ($>280 \text{ nm}$) installed in a water-cooled quartz immersion apparatus, by using a HALOS 500 W high-pressure Hg lamp as the light source. A 0.050*M* solution of **1** (0.10 mmol) was purged with ethylene for 5 min at 25°C and irradiated at a given temperature under ethylene until the enone was almost completely consumed. The reaction was monitored by TLC on silica gel. After the solvent was evaporated, the residue was purified chromatographically to give a photoadduct. The de value of photoadduct was determined by ^1H NMR spectroscopy.

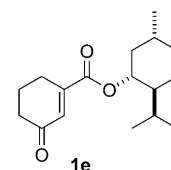
Acknowledgements

We thank Mr. S. Katao and Mr. F. Asaoma for their assistance in X-ray crystallography and ^1H NMR NOEDF spectroscopy, respectively, and

Ms. Y. Nishikawa for her help in HRMS measurements. This work was supported by a Grant-in Aid for Scientific Research on Priority Areas (B: no. 21310081 and 417) from the Ministry of Education, Culture, Sports, Science and Technology of the Japanese Government (MEXT) and the Foundation for Nara Institute of Science and Technology.

- [1] a) E. Lee-Ruff, G. C. Mladenova, *Chem. Rev.* **2003**, *103*, 1449; b) E. J. Corey, R. B. Mitra, H. Uda, *J. Am. Chem. Soc.* **1964**, *86*, 485.
- [2] a) J. D. Winkler, C. M. Bowen, F. Liotta, *Chem. Rev.* **1995**, *95*, 2003; b) M. T. Crimmins, *Chem. Rev.* **1988**, *88*, 1453; c) Y. Shimada, M. Nakamura, T. Suzuka, J. Matsui, R. Tatsumi, K. Tsutsumi, T. Morimoto, H. Kurosawa, K. Kakiuchi, *Tetrahedron Lett.* **2003**, *44*, 1401.
- [3] a) G. L. Lange, C. Decicco, S. L. Tan, G. Chamberlain, *Tetrahedron Lett.* **1985**, *26*, 4707; b) G. L. Lange, C. Decicco, M. Lee, *Tetrahedron Lett.* **1987**, *28*, 2833; c) H. Herzog, H. Koch, H.-D. Scharf, J. Runsink, *Tetrahedron* **1986**, *42*, 3547.
- [4] K. Tsutsumi, K. Endou, A. Furutani, T. Ikki, H. Nakano, T. Shintani, T. Morimoto, K. Kakiuchi, *Chirality* **2003**, *15*, 504.
- [5] a) J. Seyden-Penne in *Chiral Auxiliaries and Ligands in Asymmetric Synthesis*, Wiley, New York, **1995**; b) H. Oertling, A. Reckziegel, H. Surburg, H. J. Bertram, *Chem. Rev.* **2007**, *107*, 2136.
- [6] a) F. A. Kang, Z. Q. Yu, H. Y. Yin, C. L., *Tetrahedron: Asymmetry* **1997**, *8*, 3591; b) F. A. Kang, C. L. Yin, S. W. She, *J. Org. Chem.* **1996**, *61*, 5523.
- [7] N. Hoffmann, *Tetrahedron: Asymmetry* **1994**, *5*, 879.
- [8] a) H. M. Walborsky, L. Barash, T. C. Davis, *J. Org. Chem.* **1961**, *26*, 4778; b) H. M. Walborsky, L. Barash, T. C. Davis, *Tetrahedron* **1963**, *19*, 2333; c) K. Furuta, K. Iwanaga, H. Yamamoto, *Tetrahedron Lett.* **1986**, *27*, 4507.
- [9] a) F. Bigi, G. Casnati, G. Sartori, C. Dalprato, R. Bortolini, *Tetrahedron: Asymmetry* **1990**, *1*, 857; b) F. Bigi, G. Bocelli, R. Maggi, G. Sartori, *J. Org. Chem.* **1999**, *64*, 5004.
- [10] A. Furutani, K. Tsutsumi, H. Nakano, T. Morimoto, K. Kakiuchi, *Tetrahedron Lett.* **2004**, *45*, 7621.

- [11] K. Tsutsumi, H. Nakano, A. Furutani, K. Endo, A. Merpuge, T. Shintani, T. Morimoto, K. Kakiuchi, *J. Org. Chem.* **2004**, *69*, 785.
- [12] The calculations were performed by using the Spartan'06 software molecular modeling package for Windows available from Wavefunction, Irvine, CA.
- [13] The substrate **1e** was reported, see reference [4]. Compound **1e**: ¹H NMR (400 MHz, CDCl₃, 25°C, TMS): δ = 6.54 (s, 1H), 4.55 (m, 1H), 2.36–2.17 (m, 4H), 1.83–1.80 (m, 2H), 1.65–0.75 (m, 9H), 0.68–0.51 ppm (m, 9H).
- [14] Compound **1a**: ¹H NMR (500 MHz, CDCl₃, 25°C, TMS): δ = 7.31–7.37 (m, 3H), 7.22–7.15 (m, 2H), 6.13 (s, 1H), 4.98 (td, *J* = 11.8, 4.4 Hz, 1H), 2.31–1.98 (m, 5H), 1.89–1.82 (m, 4H), 1.70 (m, 1H), 1.49 (m, 1H), 1.33–1.14 (m, 7H), 1.06–0.84 ppm (m, 5H); **1c**: ¹H NMR (500 MHz, CDCl₃, 25°C, TMS): δ = 7.12 (d, *J* = 8.5 Hz, 2H), 6.71 (d, *J* = 8.5 Hz, 2H), 6.16 (s, 1H), 4.95 (td, *J* = 10.7, 4.3 Hz, 1H), 3.68 (s, 3H), 2.33–2.00 (m, 5H), 1.93–1.65 (m, 5H), 1.50–1.40 (m, 1H), 1.26 (s, 3H), 1.14 (s, 3H), 1.02–0.84 ppm (m, 6H); **1d**: ¹H NMR (500 MHz, CDCl₃, 25°C, TMS): δ = 8.07 (d, *J* = 9.2 Hz, 2H), 7.41 (d, *J* = 9.2 Hz, 2H), 5.92 (s, 1H), 4.95 (td, *J* = 10.7, 4.3 Hz, 1H), 2.28–2.05 (m, 5H), 1.92–1.75 (m, 5H), 1.60–1.46 (m, 1H), 1.34–1.15 (m, 7H), 1.03–0.86 ppm (m, 5H).
- [15] See the Experimental Section.
- [16] a) N. Harada, K. Nakanishi, *Circular Dichroic Spectroscopy: Exciton Coupling in Organic Stereochemistry*, University Science Books, Mill Valley, **1983**; b) N. Berova, K. Nakanishi, R. W. Woody, *Circular Dichroism Principles and Applications*, Vol. 12, 2nd ed., Wiley-VCH, Weinheim, pp. 337–342; c) M. Kasha, H. R. Rewls, M. A. E. -Bayoumi, *Pure Appl. Chem.* **1965**, *11*, 371; d) T. Furo, T. Mori, T. Wada, Y. Inoue, *J. Am. Chem. Soc.* **2005**, *127*, 8242; e) J. I. Seeman, H. Ziffer, *J. Org. Chem.* **1974**, *39*, 2444.



Received: February 18, 2010
Published online: May 12, 2010